Analytical and Numerical Tooth Contact Analysis (TCA) of Standard and Modified Involute Profile Spur Gear

Asst. Lect. Nassear Rasheid Hmoad
Department of Mechanical Engineering
College of Engineering
University of Baghdad
Nassear_machine@yahoo.com

Prof. Mohammad Qasim Abdullah
Department of Mechanical Engineering
College of Engineering
University of Baghdad
mohq1969@yahoo.com

ABSTRACT

Among all the common mechanical transmission elements, gears still playing the most dominant role especially in the heavy duty works offering extraordinary performance under extreme conditions and that the cause behind the extensive researches concentrating on the enhancement of its durability to do its job as well as possible. Contact stress distribution within the teeth domain is considered as one of the most effective parameters characterizing gear life, performance, efficiency, and application so that it has been well sought for formal gear profiles and paid a lot of attention for moderate tooth shapes. The aim of this work is to investigate the effect of pressure angle, speed ratio, and correction factor on the maximum contact and bending stress value and principal stresses distribution for symmetric and asymmetric spur gear. The analytical investigation adopted Hertz equations to find the contact stress value, distribution, and the contact zone width while the numerical part depends on Ansys software version 15, as a FE solver with Lagrange and penalty contact algorithm. The most fruitful points to be noticed are that the increasing of pressure angle and speed ratio trends to minimize all the induced stresses for the classical gears and the altered teeth shape with larger loaded side pressure angle than the unloaded side one behave better than the symmetric teeth concerning the stress reduction.

Key words: symmetric and asymmetric spur gear, contact stress.

تحليل تلامس الأسنان نظرياً وعددياً للتروس الصماء التقليدية والمعدلة ذات الجانبية الالتفافية

م.م. نصير رشيد حمود
قسم الهندسة الميكانيكية
كلية الهندسة / جامعة بغداد

أ. محمد قاسم عبدالله
قسم الهندسة الميكانيكية
كلية الهندسة / جامعة بغداد

الخلاصة

من بين كل عناصر النقل الميكانيكية المعروفة لاتزال المسننات تلعب دوراً مهيمناً خاصةً في الاعمال الثقيلة مقدمةً اداءً استثنائياً تحت الظروف المتطرفة وهو سبب كثرة الابحاث المركزة على تحسين مقاومتها لآداء دورها على اكمل وجه. يعتبر توزيع إجهادات التلامس في الاسنان واحداً من اهم العوامل المحددة لحياة المسنن وآداؤه وكفائته ومجال تطبيقه لذلك تم تحريه بعناية للمسننات ذات الجانبية المنهجية ومنح الكثير من الاهتمام لأشكال الاسنان المعدلة. الهدف من هذا العمل هو تحري تأثير زاوية الضغط ونسبة التحويل و معامل التصحيح على القيمة العظمى لإجهاد التلامس والحناية وتوزيع الإجهادات الرئيسية للمسننات الصماء المتناظرة وغير المتناظرة. اعتمد التحليل النظري معادلات (Hertz) لحساب إجهاد التلامس وتوزيعه وعرض منطقة التلامس بينما اعتمد الحل العددي برنامج Ansys النسخة الخامسة عشر لايجاد الاجهادات باستخدام خوارزمية (Lagrange- penalty). أهم النقاط المثمرة التي ينبغي ملاحظتها ان زيادة زاوية الضغط ونسبة السرع تميل لتقليل كل إجهادات المسننات التقليدية و إن الاسنان معدلة الشكل ذات زاوية تحميل اكبر من نظيرتها غير المحملة تتصرف بشكل افضل من الاسنان المتناظرة فيما يخص تقليل الإجهادات.

الكلمات الرئيسية: المسننات الصماء المتناظرة وغير المتناظرة, إجهاد التلامس.

1. INTRODUCTION

Gears have been focused on as the prime power transmission mechanical elements regarding durable and superior stress and vibration related performance. The confidence of any mechanical system is austerely related to the survival of its components under the working environment conditions such as contact, bending, and thermal stresses, vibration, fatigue and so on. The requirements placed on gear design technology are constantly increasing and need new technical solutions which are mainly related to the gear teeth shape altering aiming to reach the optimum geometrical combination that reduces the induced teeth contact and bending stresses o that, spur gear has an extensive studies regarding mathematical representation, manufacturing, transmission errors, stress analysis, wear, dynamic behavior, efficiency , and performance etc.

The most well known formulations addressing the problem of gear stresses ,Lewis equation for fillet stresses and Hertz equation for contact stresses, are derived for standard tooth profiles and show some shortage to come up with the nowadays gear design tools and manufacturing facilities which enable designer to innovate gears like never known before. Aiming to fit modern industry needs researchers, societies and companies still developing these formulations, and the latest formula for bending stress is M.Q. Abdullah equation, **Abdullah, 2012,** and AGMA equation for contact stress, **Slogén, 2013.**

It has been found that the contact stress and wear rate are expressing each other because of the intensity of contact stress play an important role in quantifying the amount of wear and vice versa the amount of wear change the involute profile by a certain distribution and lead to increase the induced contact stress with some improvements on the transmission smoothness **Farhan Muhammad et.al, 2015**. This study is focusing on the contact stress and the induced principal stresses within the tooth subsurface as the base of tooth shape optimization and simulates the studied cases numerically to compare with the mathematical results and then adopted to verify the nonstandard teeth profile results.

2. SLIDING BEHAVIOR

Pinion and gear push each other and transmit power depending on the sliding and rolling actions during the period of engagement. The maximum sliding action occurs at the tip and base of tooth regions and accompanied by heat generation, wear development, and power loss but it is unavoidable action and necessary to sustain the successive engagement of teeth. Rolling action is dominant at pitch point and accompanied by high pressure intensity without heat generation or wear setup. In general the larger sliding distance the greater wear rate and the lower vibration. It is often required to find the amount of the sliding velocity which has got a direct bearing on the amount of wear, **Maitra, 2001**. The relative sliding velocity is expressed as follows.

$$s_v = s_d \times (\omega_1 - \omega_2) \tag{1}$$

Where $\omega_1$and ω_2 are the angular speed of pinion and gear respectively, s_d is the relative sliding distance.

$$s_{d\,max} = \sqrt{Ra_1{}^2 - Rb_1{}^2} + \sqrt{Ra_2{}^2 - Rb_2{}^2} - (R_{p1} + R_{p2}) \times \sin\alpha \tag{2}$$

Where $Ra_{1,2}$ are the gear and pinion addendum radii, $Rb_{1,2}$ are the gear and pinion base radii, $R_{p1,2}$ are gear and pinion pitch radii, and α is the pressure angle.

The distribution of sliding distance and velocity is linear and identical for the flank and face portions of uncorrected tooth profiles unlike its counterpart, it is linear but with larger value for addendum than the dedendum part.

The load share between the successive teeth indicates the gear load carrying capacity which could be expressed in terms of contact ratio (CR). Higher contact ratio means larger number of gear teeth contributing power transmission leading to elongate gear life and generally it is ranging from 1.2 to 1.6 for standard applications. Working contact ratio is less than the design one due to mounting and assembly errors and that increases the vibration and coarsens the transmission process, **Tharmakulasingam, 2009.**

$$CR = \frac{s_{d\,max}}{\pi m} \tag{3}$$

Where CR is the contact ratio and m is the module.

3. HERTZ CONTACT STRESS

Due to its high intensity value compared to other stresses induced in gear teeth, contact stress has been paid a lot of attention in the design process to be the deciding factor for the determination of the requisite dimensions of gears aiming to minimize its maximum value as possible to be less than the allowable value and rearrange its distribution. In 1881 Heinrich Hertz derived his famous equation to calculate the induced contact stress between two elastic cylinders. Hertz theory assumed that the surfaces are continuous, smooth, nonconforming, frictionless, the size of the contact area is small compared to the size of the bodies, i.e., the strains associated with the deformations are small, each solid can be considered to behave as an elastic half-space in the vicinity of the contact zone, **Bhushan, 2001.**

The main shortages of this equation in gearing field are that the radius of tooth profile is not constant and it is a permanent calculation error, and the contact stress becomes infinite at the base of the profile so that it is not applicable at this point. This equation is the most dependable and accurate ever known approach simulates contact mechanism realistically and has been dealt with as the dominant equation over 100 years, where the contacting zone half width is see **Fig.1**, **Johnson 1985**

$$a = \sqrt{\frac{4F\left(\frac{1-v1^2}{E_1}+\frac{1-v2^2}{E_2}\right)}{\pi b\left(\frac{1}{r_1}+\frac{1}{r_2}\right)}} \tag{4}$$

And the maximum contact pressure is

$$P_{max.} = \frac{2F}{\pi ab} = \sigma_c \quad (5)$$

Sub. Eq. (4) in Eq. (5) the maximum contact stress will be

$$\sigma_c = \sqrt{\frac{1}{\pi} * \frac{F}{b} \frac{\left(\frac{1}{\rho_1}+\frac{1}{\rho_2}\right)}{\left(\frac{1-\nu_1^2}{E_1}+\frac{1-\nu_2^2}{E_2}\right)}} \quad (6)$$

And spreads over the contacting zone as follow

$$P = \sigma_c \sqrt{1 - \frac{x^2}{a^2}} \quad (7)$$

The principal stresses under the contacting surfaces is expressed by

$$\sigma_1 = \sigma_y = a\, P_{max}(a^2 + y^2)^{-0.5} \quad (8)$$

$$\sigma_2 = \sigma_x = \frac{P_{max}}{a} [(a^2 + 2y^2)(a^2 + y^2)^{-0.5} - 2y \quad (9)$$

$$\sigma_3 = \nu\, (\sigma_1 + \sigma_2) \quad (10)$$

any discontinuity within the contacting surfaces or sharp edges rising up the interacting pressure rapidly which is existed in case of undercut, if the teeth number is lower than the minimum number as in Eq.(11), and at the tip of any tooth without tip modification.

$$z_{min} = \frac{2}{(sin\alpha)^2} \quad (11)$$

4. INTERFERING AND TOOTH CORRECTION

The transmitted power and available space are the functional criteria for choosing gear system size which is characterized by module and tooth number. Beyond the minimum teeth number the tip of cutting tool will Remove the material from the tooth fillet region, layer after layer during the reciprocating process between the cuter and gear blank modifying the manufactured gears to have jam free engagement action, making the gear fillet and involute shape no more in tangency but intersect each other, **Litvin, 2004**. This material removal has some disadvantages such as weakening the tooth bending strength, defeat the involute profile to be shorter than its normal length, and the intersecting point of involute profile with the trochoidal fillet shape produces a sharp edge along the face width produce a high stress concentration zone. One of the most beneficial solutions to overcome the undercut problem is addendum modification by some correction factor leading to some geometrical improvements like increasing weakest section tooth width, preventing the sudden change in tooth profile and emergence of sharp edge, enlarging the pressure angle, and increasing load carrying capacity see **Fig. 2**. The amount of addendum correction factor is obeyed to

$$x = \frac{z_{min} - z}{z_{\mathrm{m}}} \tag{12}$$

5. CASE STUDY

The effect of pressure angle for symmetric and asymmetric spur gear on the induced contact stress is sought numerically and analytically. The FEM has been adopted to build up the 3-D model and analyzed the contact stress using Ansys software version 15. Hertz equation is modified to take into account the correction factor, the adjusted radius of curvature, and the working pressure angle affected by the correction are;

$$\tan\alpha_c - \alpha_c = \frac{2(x_1+x_2)}{z_1+z_2}\ \tan\alpha + \tan\alpha - \alpha \tag{13}$$

$$r_{pc} = r_p \frac{\cos\alpha}{\cos\alpha_c} \tag{14}$$

Eq.(7) must be solved numerically to get the working pressure angle equivalent to the summation of pinion and gear correction factors to evaluate the corrected pitch radius so that Eq.(4) will be

$$\sigma_c = \sqrt{0.35 * \frac{F_n}{b} \frac{\left(\frac{1}{R_{1c}\sin\alpha_c} + \frac{1}{R_{2c}\sin\alpha_c}\right)}{\left(\frac{1}{E_1} + \frac{1}{E_2}\right)}} \tag{15}$$

The general dimensions and properties of the sought models are shown in **Table 1**, the range of pressure angles are shown in **Table 2**, the applied normal load have been chosen to be 100 N and contact position is the pitch point.

7. RESULTS AND DISCUSSIONS

7.1 Analytical Results

Hertz contact stress equation have been applied directly to the proposed studied cases of 20^o and 25^opressure angles but the 14.5^o pressure angle needs some addition calculation because the minimum teeth number for such pressure angle is 32 tooth according to Eq. (11) while the current teeth number is 14 tooth i.e. gear suffers of large undercut depending upon Eq. (12) the correction factor is ($0.56\ m_o$) **Fig.2** shows the corrected and uncorrected spur gear teeth. The radius of curvature at the pitch point equal to (49 *sin α) but in the case of corrected gear the pitch point radius and the working pressure will change and could be calculated according to Eq. (13) and Eq. (14). **Table 3** represents the correction amount with its working pressure angles and corrected pitch radii.

Fig.3 relates the change in the contact zone half width distance to the variation of the pressure angle and the speed ratio. It is distinct that the increasing of the pressure angle and speed ratio plays a good role on the increasing of the contact area, because both increase the radius of curvature.

Fig.4 shows the effect of pressure angle on the contact stress, for different speed ratios, it is clear that the increasing of the pressure angle, by 20^o, reduced the contact stress by about 34%, while tripling the speed ratio decreases the contact stress by about 22%, and the cause of that is the larger angle and speed ratio means a larger contact radius of curvature leading to increase the contact zone width, i.e. the same load spread over a larger area. The other remark to be noticed is that the pressure angle sustains its effect on the contact stress but the speed ratio effect diminishes or becomes worthless after number 5 especially it is not an optional choice to enlarge the gear size by this magnitude.

Figs. 5.6,7 and 8 clarify how such high intensity contact stress flow or distributed within the tooth subsurface along the contacting teeth normal for 14.5^o, 20^o, 25^o, and 30^o pressure angle gear teeth respectively. The three principal stresses and the resulting von mises stresses have been converted to be dimensionless values, divided by the max. contact stress of the 14.5^o gear tooth i.e. 771 MPa.

Results emphasized the following facts

- The stress falls down or dissipated within (1 mm) beneath the tooth surface to be lower than one tenth of its max value, for the max. principal stresses and lower for the others.
- The first and second principal stresses equal to the maximum contact stress at the surface but the von mises stress is 0.6 of its value.
- The results confirm that the increasing of the pressure angle play a positive role on the reduction of all the induced stresses.

7.2 Finite Element Results

The different gear pairs have been modeled by Ansys software version 15 to investigate the induced static stresses and the pressure distribution within the contact area, along the contact zone half width distance and the gear face width. The models have been meshed using solid elements type brick with 20 nodes and contact elements 170 for the contact surface and 174 for the target surface, the material was chosen to be isotropic with linear behavior.

Fig.9.a, b show the contact stress distribution along the contact zone width and face width, it is obvious that the stress distribution matching that of Eq. (7) along the minor contact axis i.e. along the half contact zone distance a, but it refuted the assumption of Hertz theory about the contact stress distribution constancy along the contacting surfaces face width, such behavior is interpreted by the free end deformation trend which works as a stress relief regions. Despite this positive effect of these regions but it resize the face width to withstand against the external loads by about 0.8 of its real value and this is the counterpart negative effect, an evidence of such phenomenon is the pitting failure accurse faraway the tooth ends.

Fig. 10 represents the max. principal stress value and distribution for 14.5^o pressure angel teeth corrected by $0.1m_o$ and **Fig.10,b** corrected by $0.5m_o$, the max contact stress has been (771MPa) for the uncorrected gear as shown in **Fig.9** and reduced by about 21% due to correction factor, the modification of tooth profile by $0.56m_o$ for gear and pinion increase the pressure angle to be 23.97^o instead of 14.5^o and the pitch radius to be 51.9 mm instead of 49 mm and that lead to increasing the curvature radius, which is (R_p*sin α), to be 21.1 mm instead of 12.27 mm and that leads to increase the contact area by about 30% according to Eq.(4) so that the contact stress reduced.

Fig. 11 shows the bending stress distribution in the tension side bending zone affected by the pressure angle for symmetric spur gear. **Fig. 12** demonstrates the bending stress distribution in the tension side bending zone for asymmetric spur gear with loaded side pressure angle of 14.5^o pressure angle.

Fig.13 implies the effect of the unloaded side pressure angle variation on the max. contact stress of 14.5^o, 20^o, and $25^{o\ \text{pressure}}$ angle. It is evident that

- The increasing of the unloaded side pressure angle badly affected the max. induced contact stress
- The loaded side pressure angle must be greater than the unloaded side one for lower contact stress levels.
- The worst effect occurs for the gear of 14.5^o loaded side pressure angle.
- The unloaded pressure angle role diminishes after some value for the different three cases.

The larger unloaded pressure angle means a larger mass added to the spur gear teeth to be stiffer, leading to lower profile deformation at the contact point i.e. small contact zone area or high load intensity.

Fig. 14 relates the max. bending stresses for loaded and unloaded side of 14.5^o, 20^o, 25^o loaded side pressure angle with the variation of the unloaded side pressure angle. The following remarks could be concluded

- The lower loaded pressure angle accompanied by the larger bending stress, due to the increasing of the horizontal component of the applied load and decreasing of the tooth weakest section thickness.
- In general the compression side bending stress is higher than its counterpart of the tension side, due to the magnification of the bending compression side force by the vertical component of the applied load.
- The unloaded side pressure angle has a significant role regarding the bending stress reduction by control the weakest tooth thickness.

Fig.15 compares the analytical and numerical max. contact stress results for symmetric teeth of different pressure angles and shows a small discrepancy ranging between zero for 35^o pressure angle to 2.8% for 14.5^o which refers to the reliable FE model and boundary conditions.

8. CONCLUSIONS

Based on the whole presented theoretical and numerical results and explanation the following remarks could be concluded;

1. The use of asymmetric spur gears, with lower unloaded side pressure angle than its counterpart loaded side one, ensures low contact stress.
2. The higher pressure angle leads to lower contact and bending stress, with preservation of the first conclusion content.
3. The max. 1^{st} and 2^{nd} principal stresses have the same value of the max. contact stress at the contacting surfaces.
4. The unloaded side bending stress always prevails on that of the tension side.

REFERENCES

- Abdullah, M, Qasim, 2012, *Enhancement of Gear Drive Performance Using an Alternative Design Approach of Teeth Profile* " Doctorate dissertation, University of Baghdad, Collage of Engineering, Iraq.

- Bhushan, B ,2001, *Modern Tribology Handbook*", Volume One.

- Farhan Muhammad, Saravanan, Karuppanan Patil S. Santosh, 2015, *Frictional Contact Stress Analysis of Spur Gear by Using Finite Element Method, Journal,* Applied Mechanics And Materials.

- Johnson, L, K, 1985, *Contact Mechanics*, University of Cambridge.

- Litvin, L, Faydor, 2004, *Development of Gear Technology and Theory of Gearing*.

- Maitra, M, Gitin 2001, *Handbook of Gear Design*.

- Slogén, M, 2013, *Contact Mechanics in Gears*, Master's Thesis, Chalmers University of Technology, Sweden.

- Tharmakulasingam, R, 2009, *Transmission Error in Spur Gears: Static and Dynamic Finite- Element Modeling and Design Optimization*, Doctorate dissertation, Brunel University, United Kingdom.

NOMENCLATURES

a= Contact zone half width, mm.

b= Face width, mm.

CR= Contact ratio.

$E_{1,2}$= Gear and pinion modulus of elasticity, MPa.

F=Applied normal force, N.

m= Module, mm.

P=Contact pressure, MPa.

$r_{1,2}$= Gear and pinion profile radii at any contact point, mm.

$Ra_{1,2}$= Gear and pinion addendum radii, mm.

$Rb_{1,2}$= Gear and pinion base radii, mm.

$R_{p1,2}$= Gear and pinion pitch radii, mm.

s_v= Sliding velocity, mm/s.

s_d= Sliding distance, mm.

$x_{1,2}$= Gear and pinion correction factor, mm.

z_{min}=Min teeth number.

α= Pressure angle, degree

α_c= Corrected pressure angle, degree.

$v_{1,2}$= Gear and pinion Poisson's ratio.

$\rho_{1,2}$= Gear and pinion radii of curvature, mm.

$\sigma_{1,2,3}$= Maxrincipal stress, MPa.

σ_c= Max. contact stress, MPa.

Table 1. Dimensions and material properties, of studied models.

	Pinion	**Gear**
Teeth number	14	14
Module (mm)	7	
Correction factor (mm)	0.5*m	
Face width (mm)	1	
Height (mm)	2.25*m	
Fillet radius (mm)	0.25*m	

Modulus of elasticity GN/m^2	200
Poison's ratio	0.3

Table 2. Rang of pressure angles.

Loaded side pressure angle (degree)	14.5	20	25
Unloaded side pressure angle (degree)	14.5	14.5	14.5
	18	18	18
	20	20	20
	22	22	22
	25	25	25
	28	28	28

Table 3. Corrected profile pressure angle and pitch radius for 14.5^o pressure angle gear.

Correction factor (x)	0	0.1	0.2	0.3	0.4	0.5	0.56
Working pressure angle	14.5	17.13052	19.10514	20.71728	22.09404	23.30346	23.9666
Corrected pitch radius	49	49.64152	50.20452	50.71885	51.19888	51.65295	51.91523

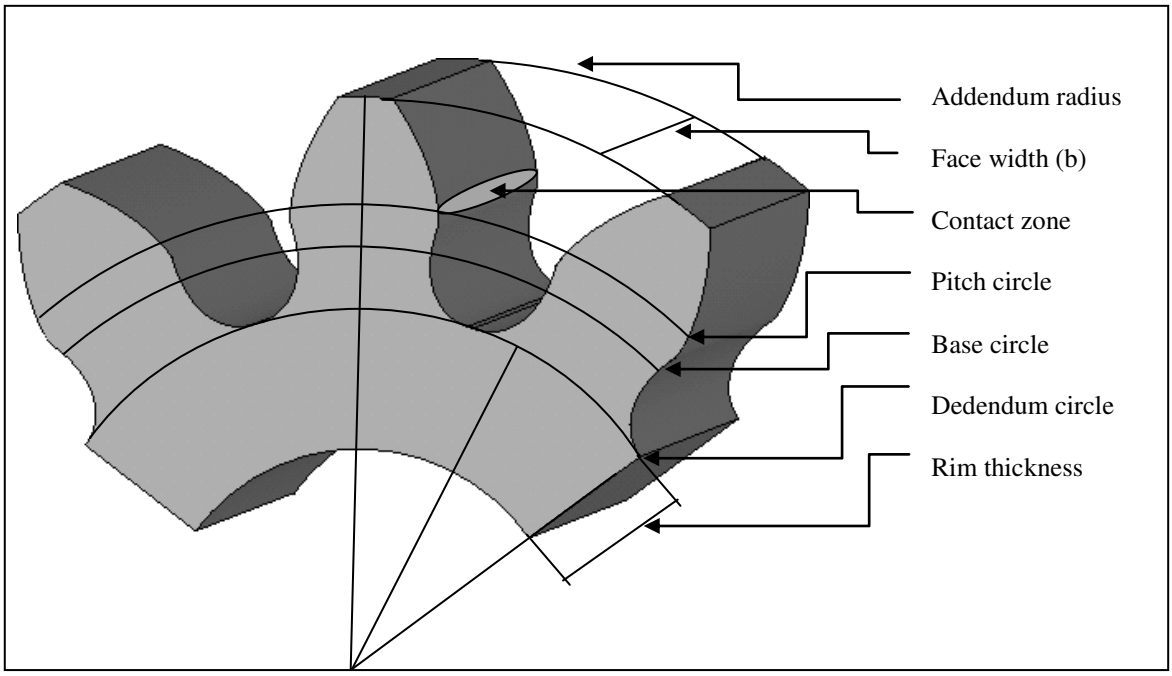

Figure 1. Geometry and main dimensions of spur gear teeth, $\alpha=20^o$, $m_o=7$ mm, Z=10 teeth.

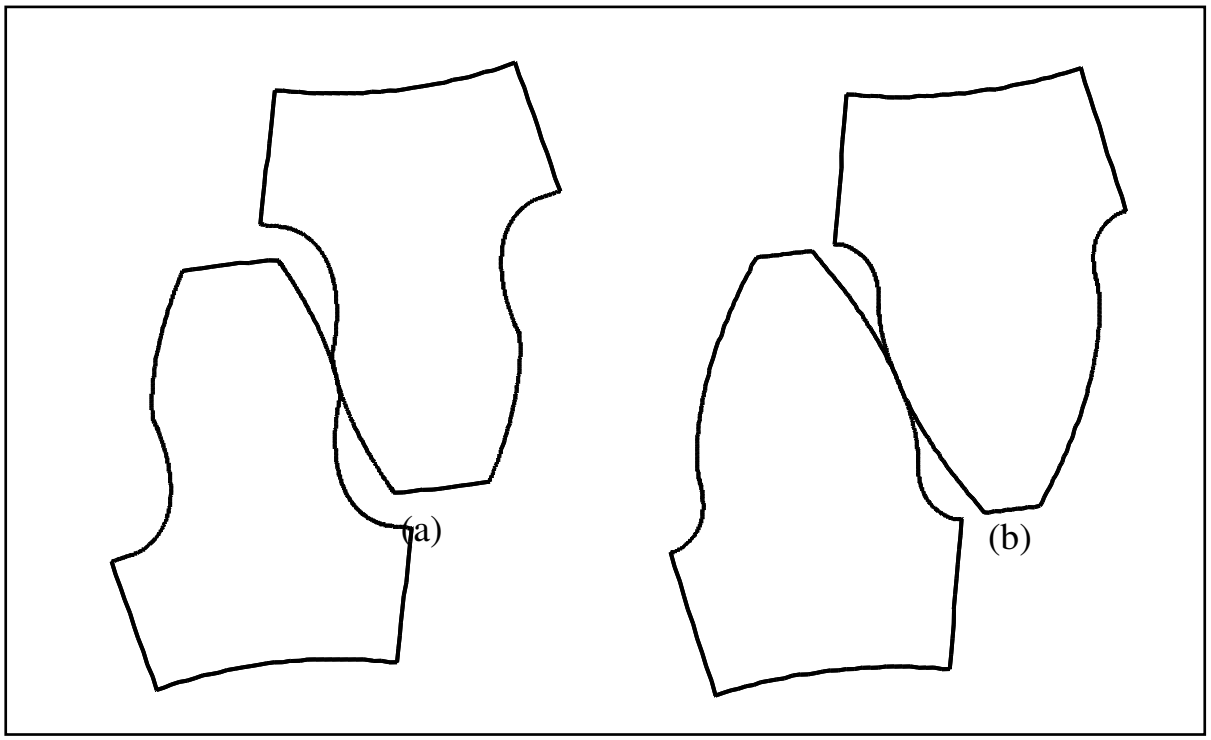

Figure 2. The effect of correction factor on the tooth shape, both have 7mm module and 14 teeth for gear and pinion . (a) Uncorrected teeth, (b) Corrected teeth by 0.5 correction factor.

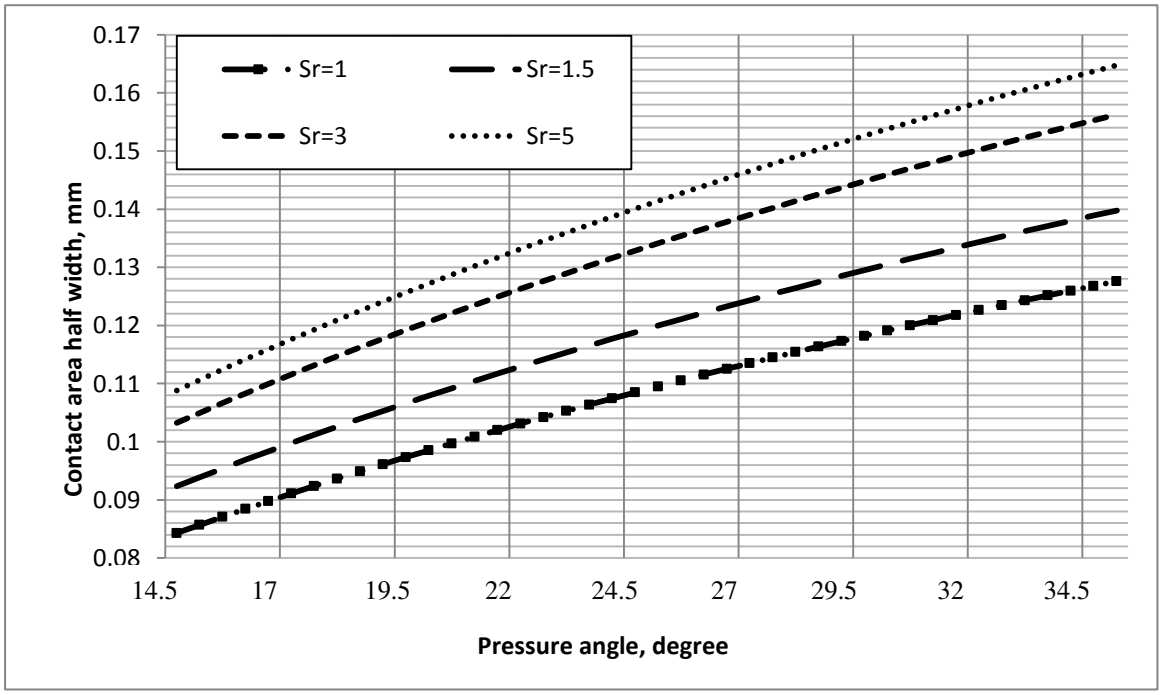

Figure 3. The effect of the pressure angle and speed ratio variation on the contact half width distance.

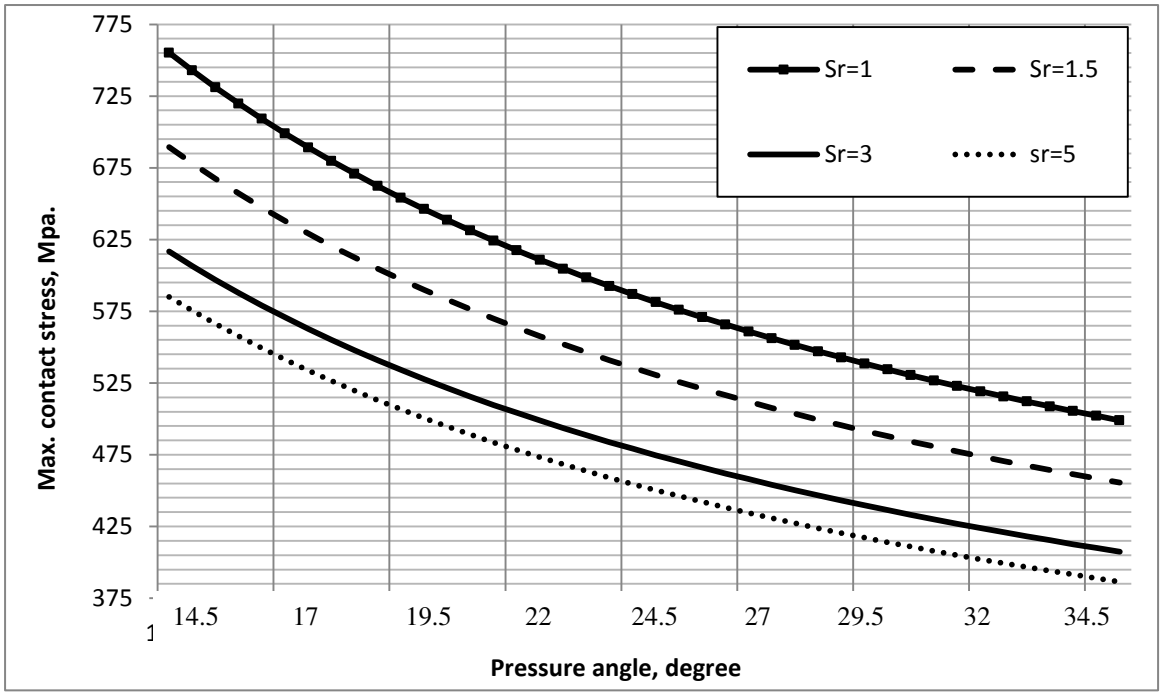

Figure 4. The Role of the pressure angle variation on the max. contact stress for different speed ratios.

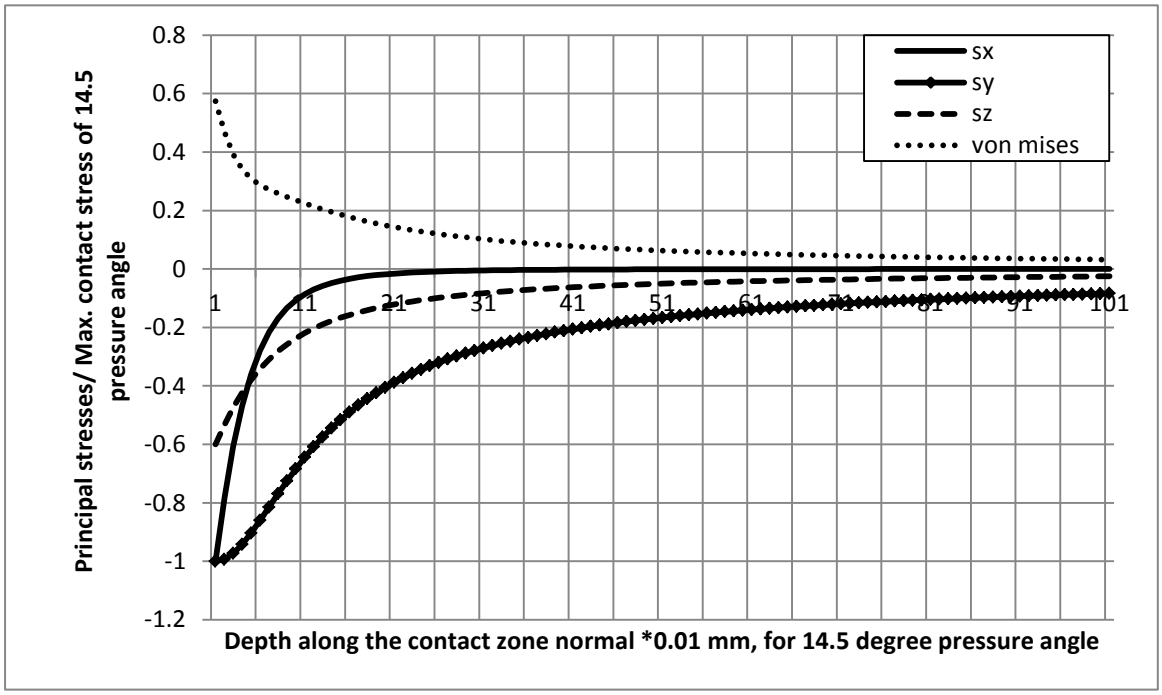

Figure 5. The dimensionless different stresses distribution along the contacting surfaces normal, the pressure angle is 14.5°.

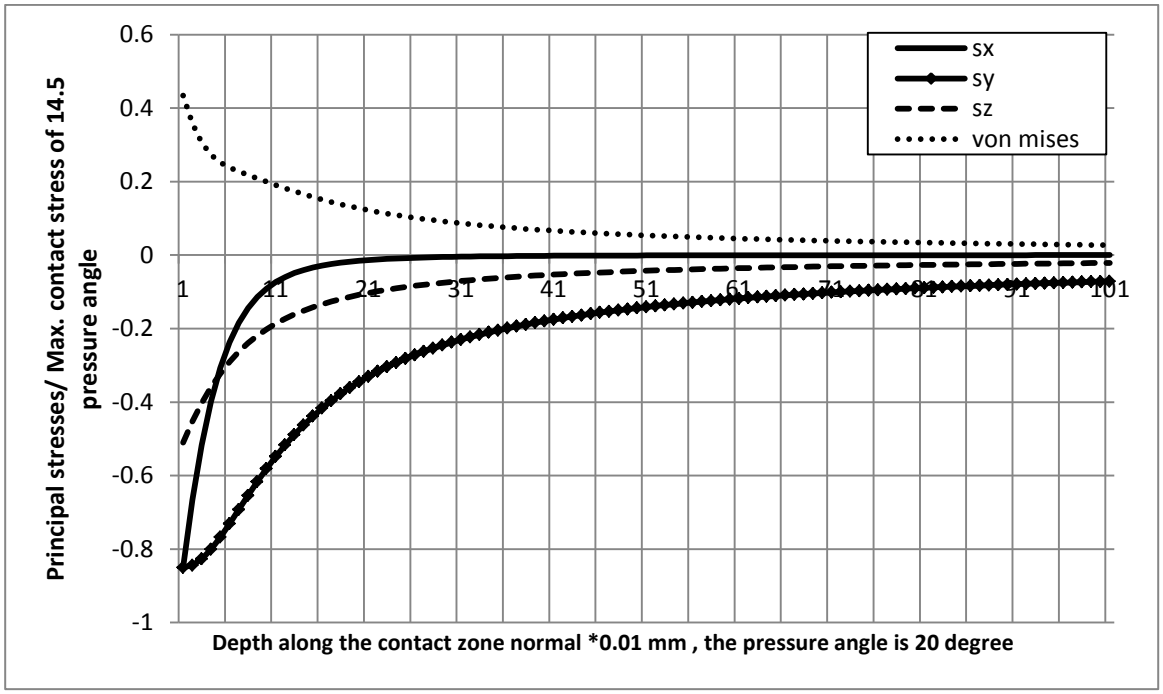

Figure 6. The dimensionless different stresses distribution along the contacting surfaces normal, the pressure angle is 20°.

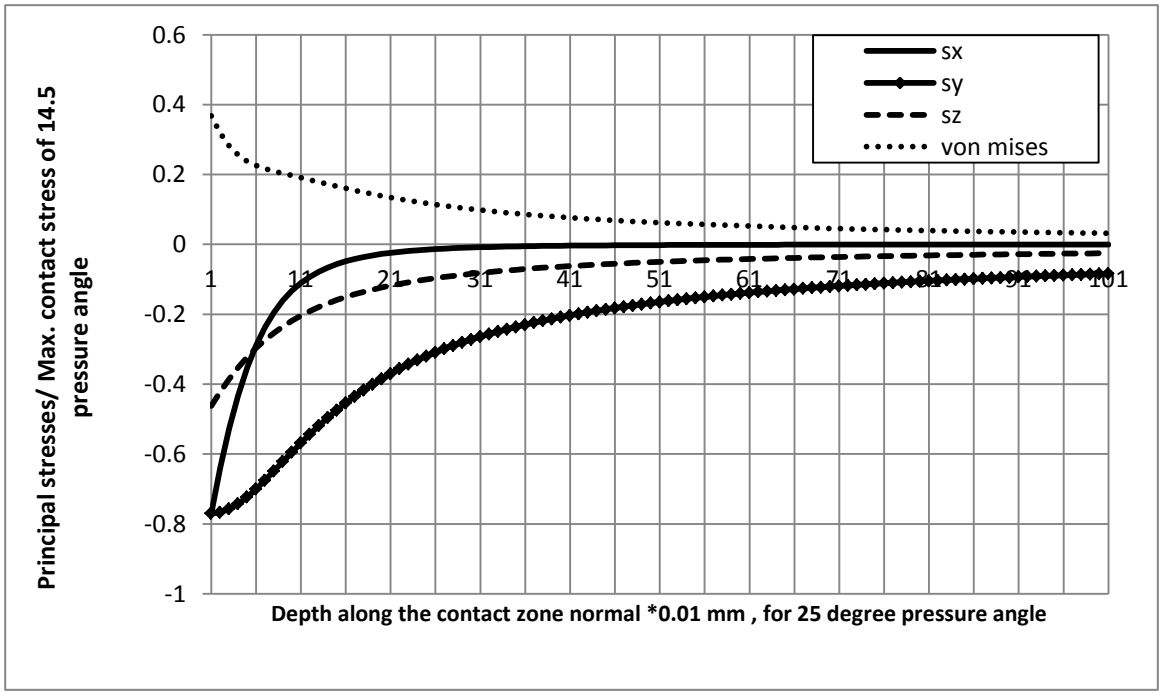

Figure 7. The dimensionless different stresses distribution along the contacting surfaces normal, the pressure angle is 25°.

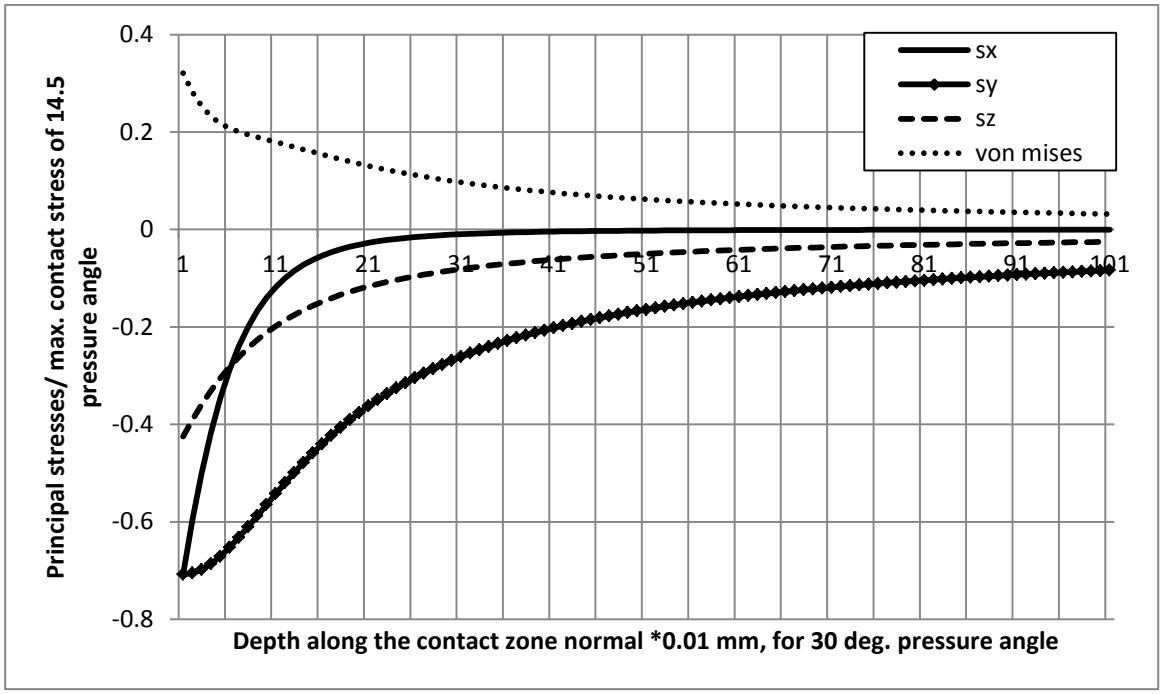

Figure 8. The dimensionless different stresses distribution along the contacting surfaces normal, the pressure angle is 30^{o}.

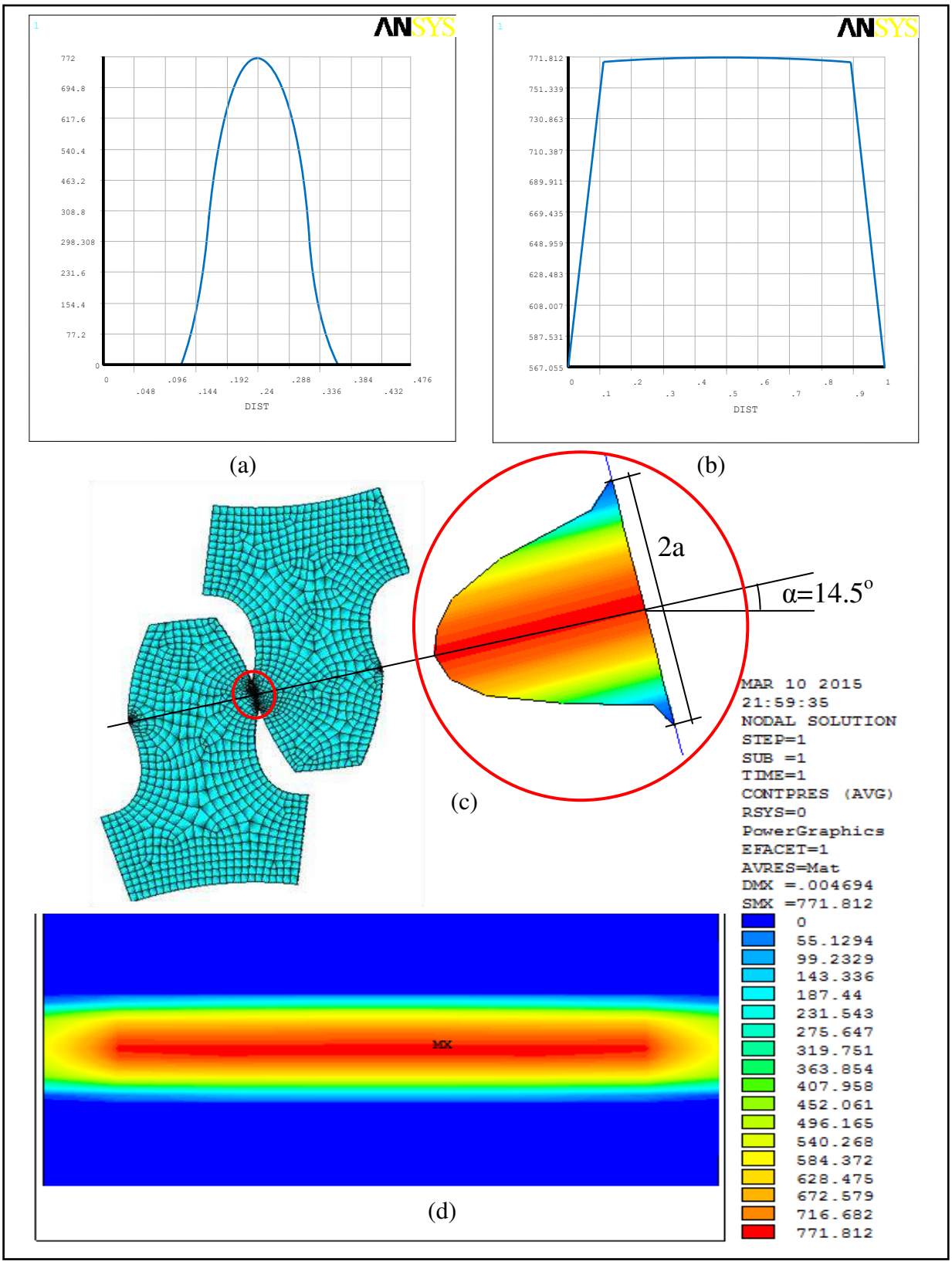

Figure 9. Contact stress distribution of symmetric spur gear of 14.5° pressure angle, (a) Along contact zone minor axis (a), (b) Along major axis (face width), (c) Teeth in mesh at pitch point, (d) Contact stress pattern in the contact zone.

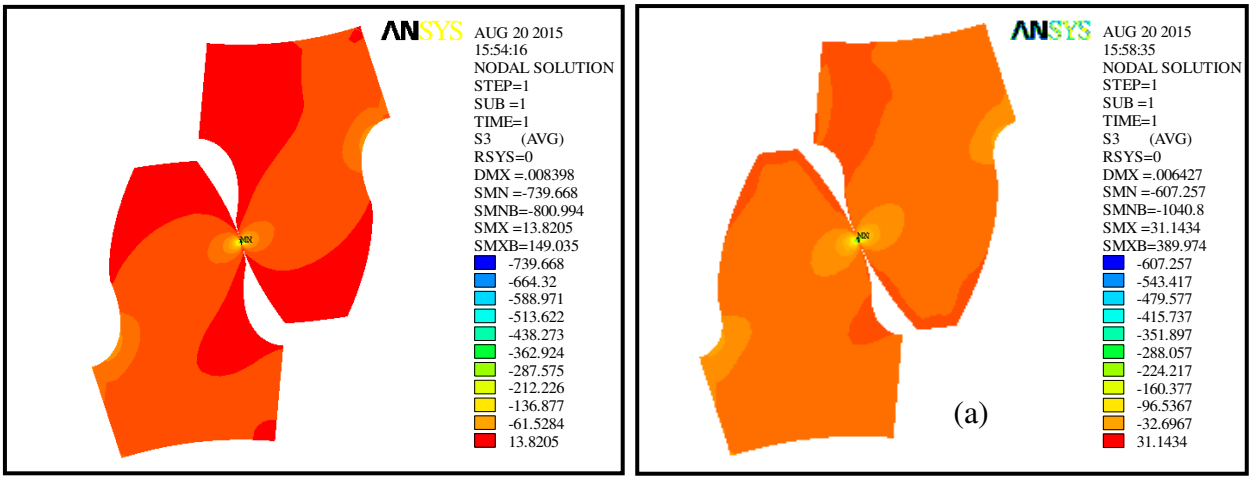

Figure 10. Max. principal stress for 14.5° pressure angle involute profile. (a) Corrected by 0.1 m_o. (b) corrected by 0.5 m_o.

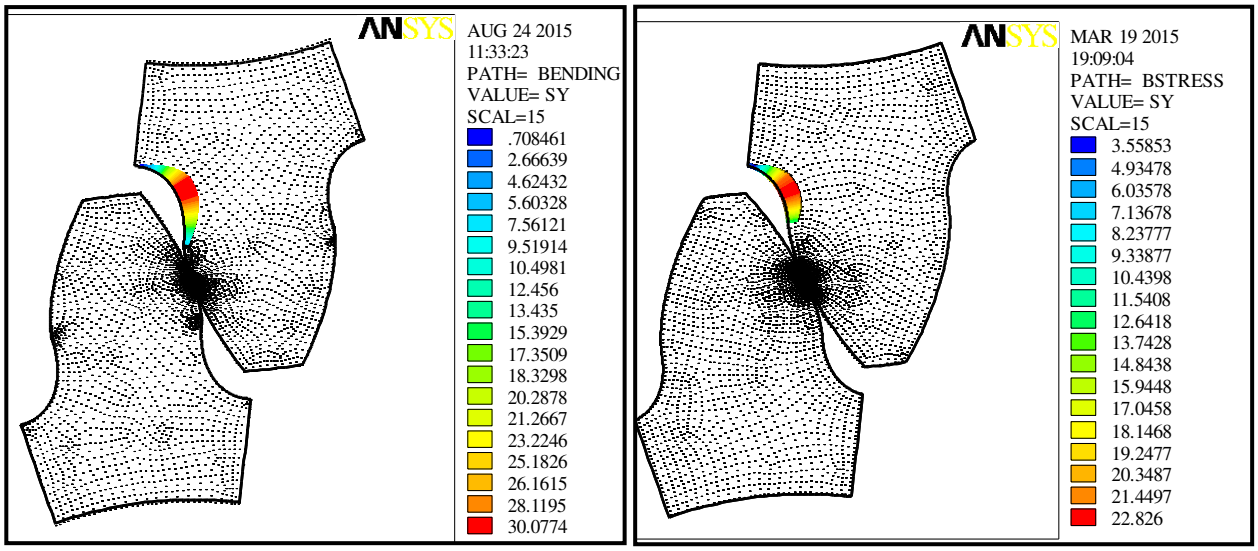

Figure 11 Max. bending stress for symmetric spur gear with (a) 20° pressure angle (b) 25° pressure angle

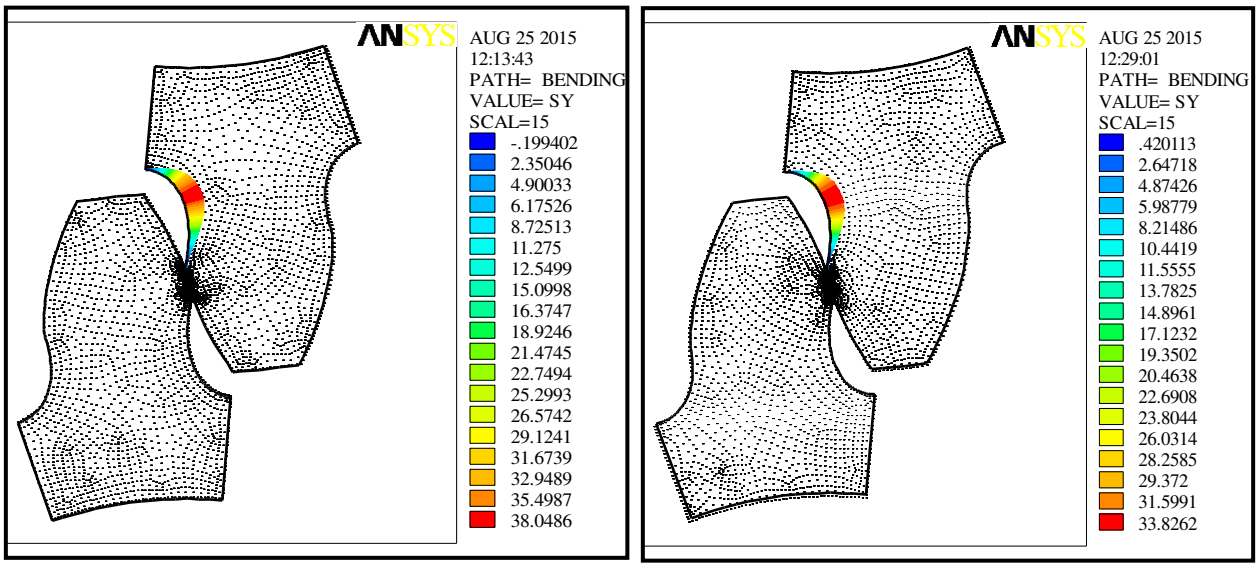

Figure 12. Max. bending stress for asymmetric spur gear with 14.5° loaded side and (a) 20° unloaded pressure angle (b) 25° unloaded pressure angle.

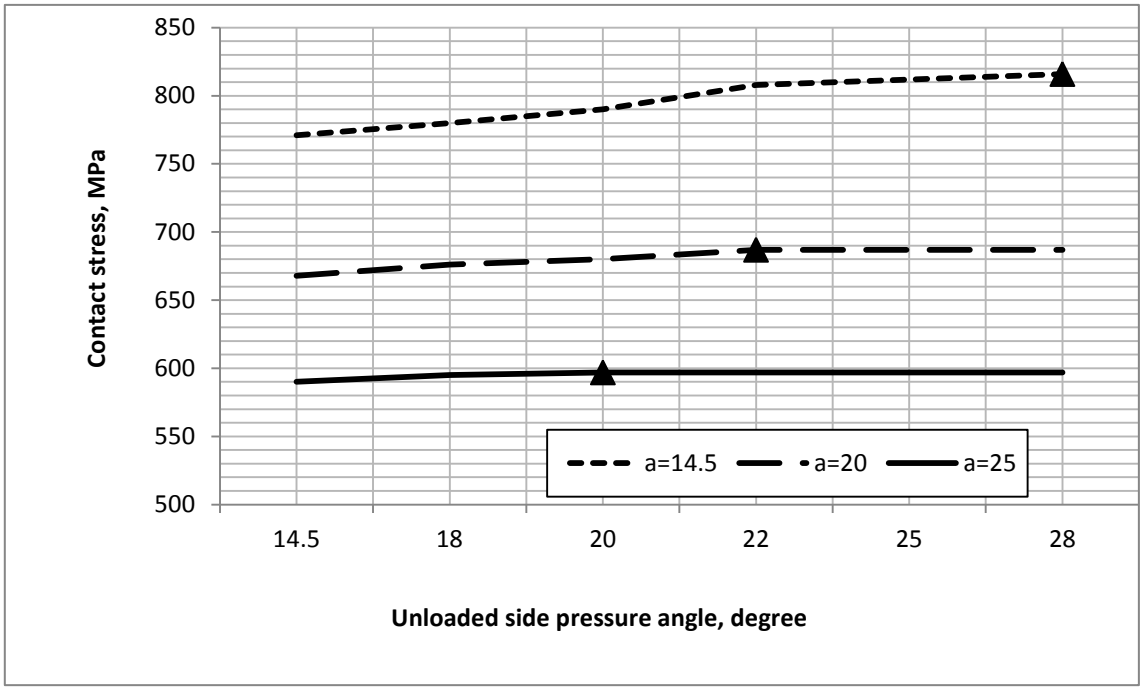

Figure 13. Max. contact stress for asymmetric spur gear with unloaded pressure side angle variation.

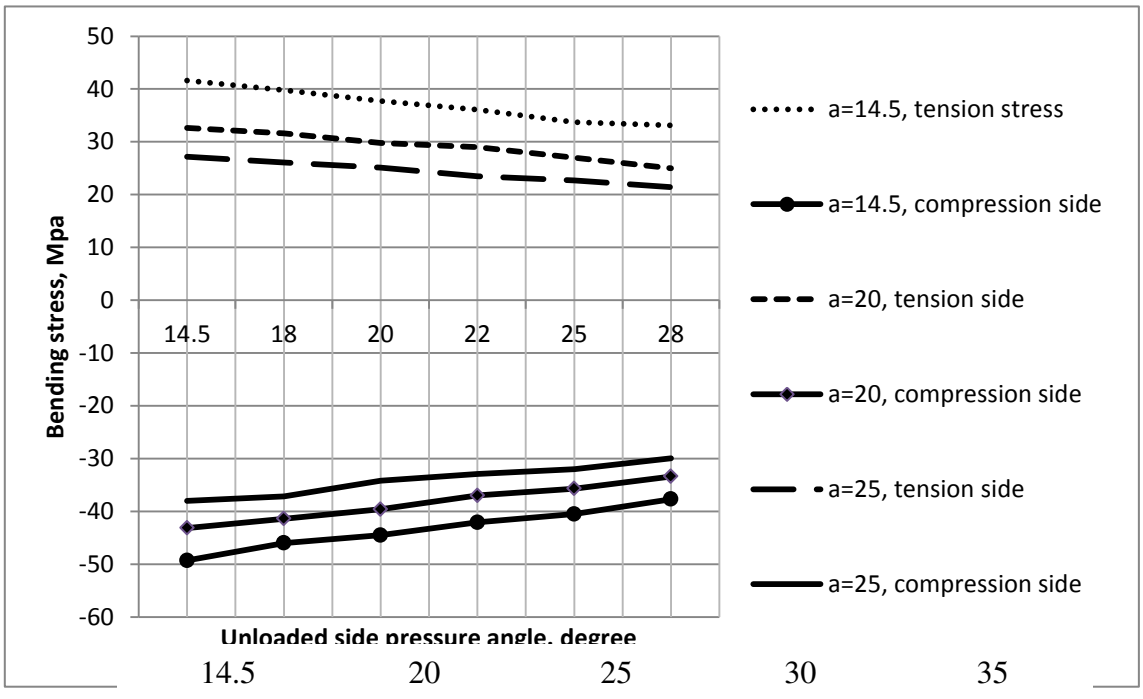

Figure 14. Max. bending stress for asymmetric spur gear with unloaded side pressure angle variation.

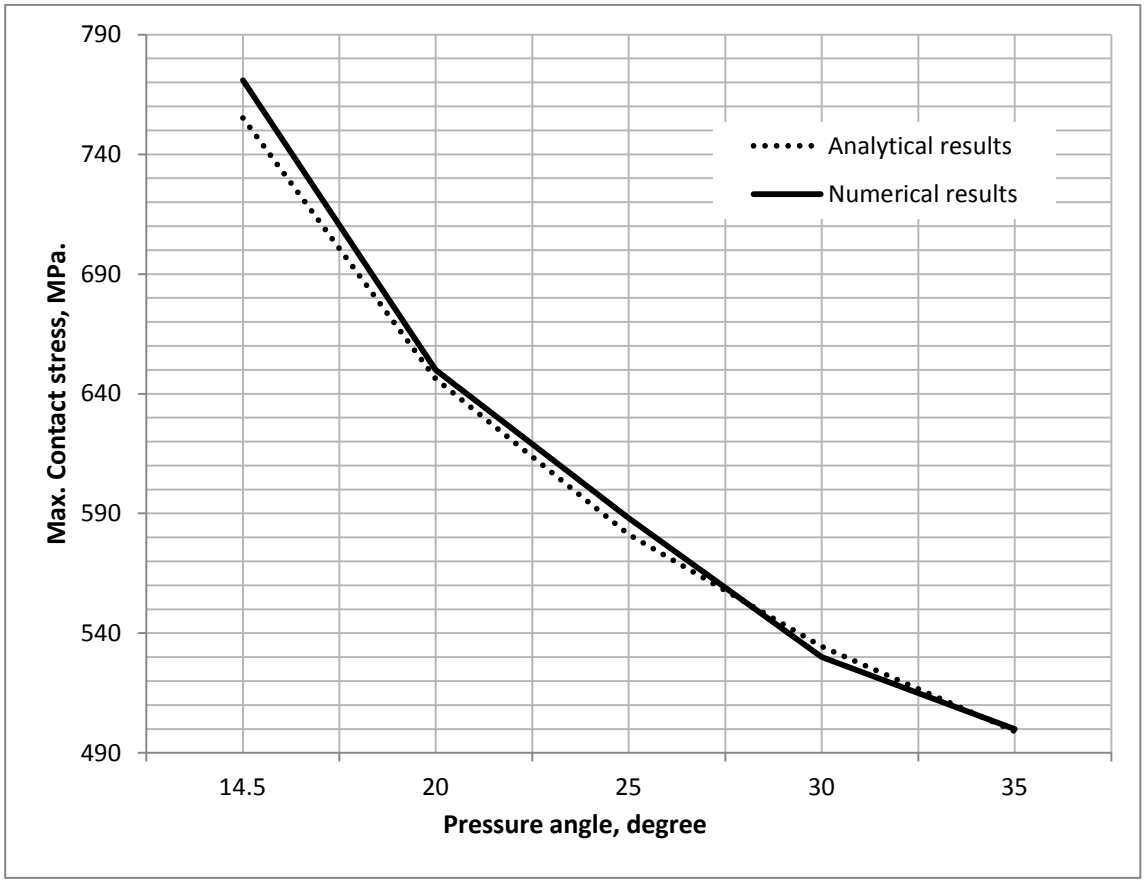

Figure 15. Analytical and numerical max. contact stress results for symmetric teeth.